

Dilithium zirconium hexafluoride Li_2ZrF_6 at high pressures: A new monoclinic phase

Andrzej Grzechnik^{a,*}, Vladimir Dmitriev^b, Hans-Peter Weber^{c,d}

^a *Departamento de Física de la Materia Condensada, Universidad del País Vasco, Apdo. 644, E-48080 Bilbao, Spain*

^b *Swiss-Norwegian Beamlines, European Synchrotron Radiation Facility, B.P. 220, F-38043 Grenoble cedex, France*

^c *Laboratoire de Cristallographie, EPFL/SB/IPMC/LCR, Swiss Federal Institute of Technology, CH-1015 Lausanne, Switzerland*

^d *ACCE, Grand Vivier, F-38960 St Aupre, France*

Received 27 May 2005; revised 23 August 2005; accepted 8 September 2005

Abstract

Dilithium zirconium hexafluoride, Li_2ZrF_6 ($P\bar{3}1m$, $Z=1$), is studied at high pressures using synchrotron angle-dispersive X-ray powder diffraction in a diamond anvil cell at room temperature. At atmospheric conditions, it has a structure with all the cations octahedrally coordinated to fluorine atoms. Above 10 GPa it transforms reversibly to a new polymorph ($C2/c$, $Z=4$), in which the coordination polyhedron of the Zr atoms is a distorted square antiprism, while the Li atoms are in the octahedral coordination. The LiF_6 octahedra form layers parallel to (100) that are connected by zig-zag chains of the edge-sharing Zr polyhedra running in the [001] direction. The relative change in volumes per one formula unit for both polymorphs is 6% at 11.8 GPa. The relations to other A_2BX_6 -type structures are discussed.

© 2005 Elsevier Ltd. All rights reserved.

Keywords: A. Inorganic compounds; C. High pressure; C. X-ray diffraction; D. Crystal structure; D. Phase transitions

1. Introduction

At atmospheric pressure, dilithium zirconium hexafluoride Li_2ZrF_6 ($P\bar{3}1m$, $Z=1$) has a structure in which all the cations are octahedrally coordinated to fluorine atoms [1,2]. The ZrF_6 octahedra share corners with two LiF_6 octahedra that share edges with one another. This structure with a hexagonal close packing of the anions could be considered as a layered one, with one-third of octahedral sites in one slab filled with the Zr atoms and two-thirds in the next occupied by the Li atoms [3].

Several structural types can easily be derived from Li_2ZrF_6 ($P\bar{3}1m$, $Z=1$) by shifting or removing the cations [3,4]. Galy and Anderson [5] proposed simple transformation mechanisms of the Li_2ZrF_6 , trirutile ($P4_2/mnm$, $Z=2$), Na_2SiF_6 ($P\bar{3}1m$, $Z=3$), and columbite FeNb_2O_6 ($Pbcn$, $Z=4$) structure types at high pressures through cation rearrangements in the anionic array. They also constructed a tentative pressure–temperature phase diagram for the ternary compounds of the general formula A_2BX_6 . Accordingly, the Li_2ZrF_6 structure would be a high-pressure variant of the trirutile type. Moreover, the A_2BX_6

materials would be expected to transform at high pressures to the columbite FeNb_2O_6 structure that is an ordered analogue of the $\alpha\text{-PbO}_2$ type ($Pbcn$, $Z=4$). In each of these structures, all the cations are octahedrally coordinated to anions [3–6]. The transformations trirutile $\rightarrow \text{Li}_2\text{ZrF}_6$ or $\text{Na}_2\text{SiF}_6 \rightarrow \text{Li}_2\text{ZrF}_6$ would correspond to the substitution of the M' atoms in the $\text{LiM}'M''\text{F}_6$ fluorides at atmospheric conditions. The $\text{LiM}'M''\text{F}_6$ compounds ($M'' = \text{Al, Ga, V, Cr, Fe}$) have the trirutile or Na_2SiF_6 structures at atmospheric conditions when the M' atoms ($M' = \text{Mg, Mn, Co, Ni, or Zn}$) are relatively small, while the colquiriite structure ($P\bar{3}1c$, $Z=2$), an ordered variant of the Li_2ZrF_6 type ($P\bar{3}1m$, $Z=1$), occurs when the M' atoms are Ca or Sr ($M'' = \text{Al, Ga, or Cr}$) [7,8].

The phase transitions trirutile $\rightarrow \text{Li}_2\text{ZrF}_6$ or $\text{Na}_2\text{SiF}_6 \rightarrow \text{Li}_2\text{ZrF}_6$ are also analogous to the ones for the AX_2 compounds as the rutile-type phases transform to the $\alpha\text{-PbO}_2$ structure at high pressures [3,6]. Sekino et al. [9] prepared a series of $\text{LiTiM}^{2+}\text{F}_6$ ($M^{2+} = \text{Mn, Fe, Co, or Ni}$) compounds at 1.5–7.0 GPa and 973–1473 K. The low-pressure phases belonged to the trirutile type. The high-pressure phases indeed crystallized in the Na_2SiF_6 -type structure for LiTiMnF_6 and in the PbSb_2O_6 -type (or the Li_2ZrF_6 -type [10]) structure for $M^{2+} = \text{Fe, Co, or Ni}$.

The Rietveld refinement of the high-pressure high-temperature polymorph of Li_2ZrF_6 similar to the Li_2TbF_6 -type

* Corresponding author. Tel.: +34 946013275; fax: +34 946013500.

E-mail address: andrzej@wm.lc.ehu.es (A. Grzechnik).

structure ($P2_1/c$, $Z=4$) has been reported recently [11]. In this new structure synthesized at 11 GPa and 1063 K and investigated at its quenched form, the zirconium atoms are eight fold coordinated to the fluorine atoms. The polyhedra can be described as edge-sharing bicapped trigonal prisms along the a -axis, with the Li^{+1} cations at two non-equivalent sites between the Zr–F chains. The Li–F coordination polyhedra at both Li^{+1} sites are square pyramids. These pyramids are joined by corners to form slabs in the (a,b) plane. The main difference between the structures of Li_2ZrF_6 and Li_2TbF_6 [12], both $P2_1/c$ and $Z=4$, is that in the latter the Li atoms are five and six fold coordinated to fluorines, respectively. The LiF_5 square pyramids are connected by corners into infinite chains along the b -axis. The LiF_6 distorted octahedra form layers in the (b,c) plane. The coordination polyhedra around the Tb atoms in Li_2TbF_6 [12] could alternatively be considered as distorted Archimedian antiprisms. Such a description allows for a comparison of the Li_2TbF_6 structure with the one of the γ - Na_2UF_6 type ($Immm$, $Z=2$), derived from the ordered fluorite structure [12]. The cubes around the U atoms correspond to the Archimedian antiprisms in Li_2TbF_6 due to displacements of fluorines in the (a,c) planes.

Our further interest in the high-pressure behaviour of Li_2ZrF_6 arises from the fact that it is a disordered archetype of the colquiriite $\text{LiM}'\text{M}''\text{F}_6$ compounds ($P\bar{3}1c$, $Z=2$; $\text{M}' = \text{Ca}$ or Sr ; $\text{M}'' = \text{Al}$, Ga , or Cr) considered for optical applications [7, 13,14]. The understanding of pressure-induced phase transitions and structures of the A_2BX_6 materials could be improved by in situ investigations of the transformations, involving the changes in coordination spheres of the cations and packing of the anions. This study is thus focused on dilithium zirconium hexafluoride Li_2ZrF_6 investigated at high pressures and room temperature in a diamond anvil cell using synchrotron angle-dispersive X-ray powder diffraction. The structural features of the Li_2ZrF_6 polymorphs and the high-pressure high-temperature systematics of the A_2BX_6 -type compounds are then examined.

2. Experimental

A finely ground sample of Li_2ZrF_6 , previously studied in Ref. [9], was loaded into diamond anvil cells with argon as a pressure transmitting medium. Angle-dispersive powder X-ray diffraction patterns were measured at room temperature on the Swiss-Norwegian Beamlines at the European Synchrotron Radiation Facility (BM1A, ESRF, Grenoble, France). Monochromatic radiation at 0.71998 Å was used for data collection on image plate (MAR345). The images were integrated using the program FIT2D [15] to yield intensity versus 2θ diagrams. The ruby luminescence method [16] was used for pressure measurements.

3. Data analysis

Diffraction patterns of Li_2ZrF_6 at different pressures are shown in Fig. 1. Up to 9.6 GPa, the stable structure is $P\bar{3}1m$ ($Z=1$) [1–3]. Above 10.0 GPa, the structure transforms to

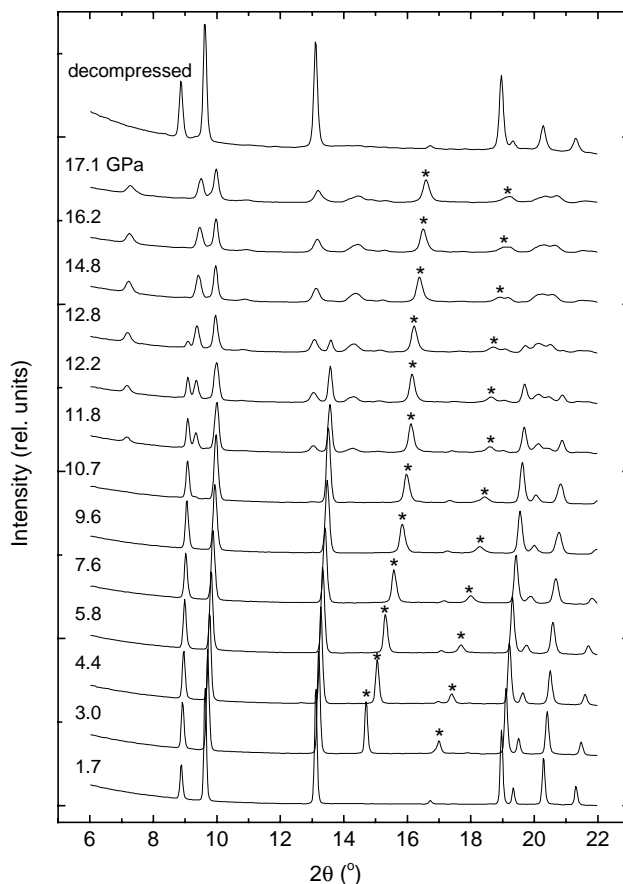


Fig. 1. Selected X-ray powder patterns of Li_2ZrF_6 at different conditions with argon as a pressure transmitting medium ($\lambda=0.71998$ Å). Reflections due to argon are marked with stars.

another modification. The lower and higher pressure phases coexist at least up to 17.1 GPa, the highest pressure reached in this study. There are no other changes in the powder patterns that could be associated with the formation of the $P2_1/c$ ($Z=4$) polymorph previously synthesized at high temperatures above 7 GPa and studied in its quenched phase [11]. Also, the calculated patterns assuming the $P2_1/c$ structural model [11] do not match the patterns observed above 10 GPa, unambiguously indicating a presence of a new polymorph of Li_2ZrF_6 . The pressure-induced phase transition is fully reversible upon decompression, as one can easily deduce from inspection of Fig. 1. The pattern collected at 14.8 GPa on compression was used for indexing with the observed reflections up to $2\theta=22^\circ$. The reflections were indexed using the program DICVOL91 [17] with a monoclinic unit cell: $a=9.651(4)$ Å, $b=7.611(2)$ Å, $c=4.986(2)$ Å, $\beta=114.78(3)^\circ$, $V=332.5$ Å³, $M(20)=7.7$, $F(20)=16.2$ (0.0159,62). The systematic absences indicated that the space group is $C2/c$ ($Z=4$) [18].

The pressure dependence of the lattice parameters and unit-cell volumes in the low- and high-pressure polymorphs of Li_2ZrF_6 is shown in Fig. 2. The volumes of the monoclinic cells ($C2/c$, $Z=4$) are normalized by a factor of 4. The compression data for the $P\bar{3}1m$ ($Z=1$) structure could be fitted up to 12.8 GPa by a Birch equation of state, giving a zero-pressure bulk modulus $B_0=80\pm 5$ GPa, a first pressure derivative of

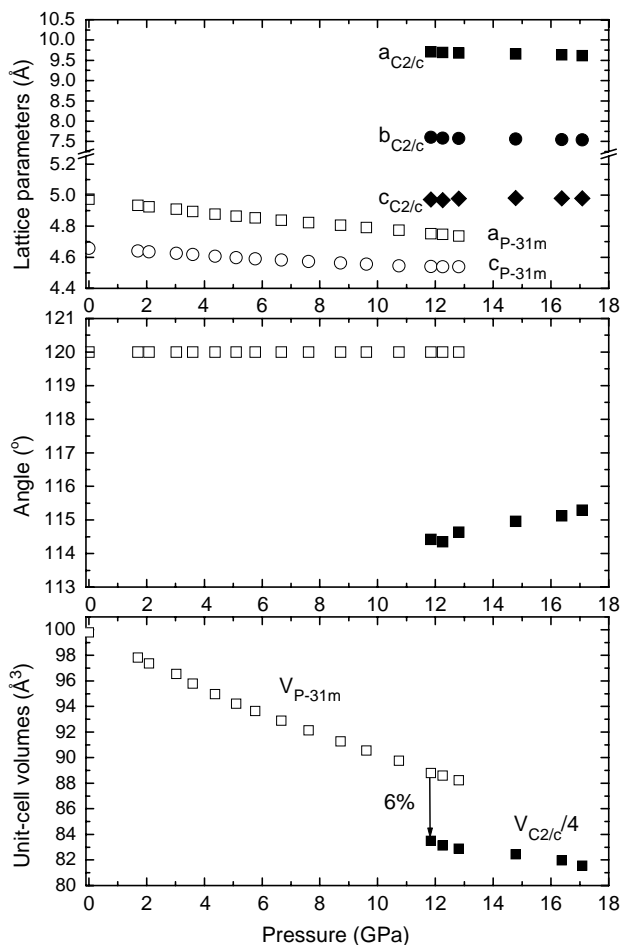


Fig. 2. Pressure dependence of unit-cell parameters and volumes in Li_2ZrF_6 . Open and full symbols stand for the $P\bar{3}1m$ ($Z=1$) and $C2/c$ ($Z=4$) polymorphs, respectively. The unit cell volumes of the monoclinic phase are divided by a factor of four. The relative volume change at 11.8 GPa is 6%.

the bulk modulus $B' = 4.22 \pm 0.87$, and a unit-cell volume at ambient pressure $V_0 = 99.8 \pm 0.2 \text{ \AA}^3$. There is a discontinuity in the pressure evolution of the unit-cell volumes at the transition $P\bar{3}1m \rightarrow C2/c$ with a relative volume change of 6% at 11.8 GPa. This result shows that the phase transformation is of first order and that major structural rearrangements in the crystal structure of Li_2ZrF_6 are to be expected above 10 GPa. The lattice parameters of the sample at ambient conditions before compression and after decompression are $a = 4.952(2) \text{ \AA}$, $c = 4.6508(7) \text{ \AA}$ and $a = 4.953(3) \text{ \AA}$, $c = 4.653(2) \text{ \AA}$, respectively [18].

The monoclinic unit cell was used in the program Endeavour [19] to solve the structure of Li_2ZrF_6 at 14.8 GPa with the global minimization method. The program was run in space group $C2/c$ with the unit cell containing four Zr cations and 24 F anions. The Li^{+1} cations were not included as their positions cannot be reliably found in the presence of the heavy Zr cations. The solutions obtained with the program Endeavour [19] yielded a crystal structure with the Zr atoms occupying the 4e sites (the positional parameters 0,y,0.25). The fluorine atoms are distributed in three non-equivalent general 8f sites (x,y,z). A topological analysis of

the globally optimized ZrF_6^{-2} sublattice was carried out using the program DIRICHLET of the TOPOS package [20]. Voronoi-Dirichlet polyhedra (VDP) for the first coordination spheres of the fluorine sublattice were constructed to determine its geometric and topological characteristics. Each of the three non-equivalent fluorine atoms was chosen in turn to be at the origin of the sublattice in the search for the VDP vertices that represent the voids in the crystal structure, i.e. in the anionic F^{-1} sublattice. The globally optimised coordinates of the Zr atoms were easily identified as some of the VDP vertices. The coordinates of the remaining VDP vertices and their connectivities, i.e. distances between the voids and the F^{-1} ions were further examined to obtain atomic coordinates for the lithium atoms. In the ZrF_6^{-2} sublattice the coordination polyhedra of the Zr atoms are distorted square antiprisms, forming zig-zag chains of the in the [001] direction. Hence, to ensure a proper distribution of all the cations [21], it was assumed in the search for the lithium atoms that they would occupy the general sites 8f with the positional parameters x and y close to 0.25 and 0.5, respectively. Subsequently, a set of four voids, for which the hypothetical Li–Li and Li–Zr distances in the cationic sublattice as well as the hypothetical Li–F bond lengths were crystallographically acceptable [20,21], turned out to be the ones with the octahedral coordination to the F atoms. The respective x , y , and z positional parameters of these voids were then averaged to give one position of the lithium atoms in the structural model for Li_2ZrF_6 ($C2/c$, $Z=4$) at 14.8 GPa.

The complete Li_2ZrF_6 structural model, i.e. the globally optimised ZrF_6^{-2} substructure and the Li^{+1} cations from the crystal topology considerations, was then used for the structure refinement against the observed pattern at 14.8 GPa with the Rietveld method using the program GSAS [22] (Fig. 3). The best fit was obtained at $R_{\text{wp}} = 19.56\%$, $R_p = 9.91\%$, $\chi^2 = 1.74$, and $R(F^2) = 6.26\%$ (the residuals R_{wp} and R_p have been calculated with the background eliminated, see the GSAS manual). The model contained a set of predefined distances between atoms, their corresponding standard deviations, and a weighting factor in order to add new ‘observables’ to the refinement. The starting minimal distances were 2.20(1) Å for F–F, 1.80(1) Å for Li–F, and 1.90(1) Å for Zr–F. The refined variables were: atomic positions, the isotropic thermal parameters for the Zr atom $U_i/U_e \times 100 = 0.3(1)$, one contracted isotropic thermal parameter for all three non-equivalent F atoms $U_i/U_e \times 100 = 4.2(8)$, lattice parameters, scale factor, and Stephens profile function [23]. The fractional coordinates for all the atoms and selected interatomic distances are given in Table 1.

4. Discussion

The pressure-induced structure of Li_2ZrF_6 occurring above 10 GPa at room temperature ($C2/c$, $Z=4$) is based on a near-hexagonal close-packing of the fluorine atoms like the rutile structure (Table 1 and Fig. 4). The coordination polyhedron of Zr is a distorted square antiprism with Zr–F distances from 1.89 to 2.15 Å (Table 1). The Li atoms are in the deformed

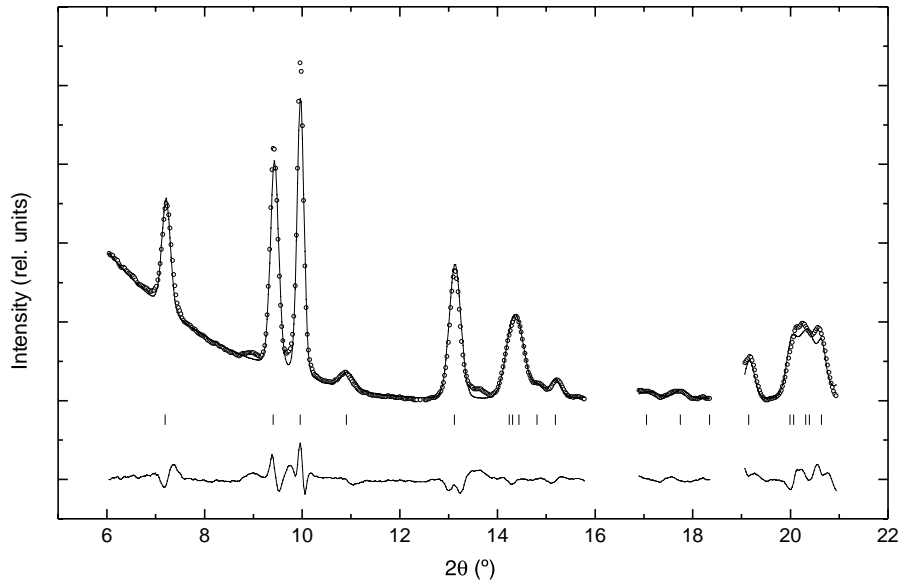


Fig. 3. Observed, calculated, and difference X-ray powder patterns for Li_2ZrF_6 ($C2/c$, $Z=4$) at 14.8 GPa as obtained after the final Rietveld refinement ($\lambda=0.71998$ Å). Vertical markers indicate the positions of Bragg reflections. The 2θ regions 15.8–16.9° and 18.35–19.06°, in which two reflections due to argon are observed, were excluded from the Rietveld refinement. Broad features at about $2\theta=8.9^\circ$ and $2\theta=13.6^\circ$ are the traces of the low-pressure phase ($P\bar{3}1m$, $Z=1$), i.e. the (001) and (101) reflections, respectively.

octahedral coordination with the Li–F distances from 1.74 to 2.19 Å. The LiF_6 octahedra share their edges and form layers parallel to (100). They are connected by zig-zag chains of the edge-sharing Zr coordination polyhedra running in the [001] direction.

At atmospheric pressure, the coordination number of the Zr atoms with respect to the fluorine atoms in fluorides is 6, 7, or 8, and the corresponding coordination polyhedra are ZrF_6 octahedra, ZrF_7 pentagonal bipyramids or monocapped trigonal prisms, or ZrF_8 square antiprisms, dodecahedra (bidisphenoids), or bicapped trigonal prisms, respectively [24]. Serezhkin et al. [25] have analyzed the geometric characteristics of the resulting Voronoi-Dirichlet polyhedra around the zirconium atoms. They have found that the volumes of the VD polyhedra are independent of the coordination number and the actual shape of the coordination polyhedron. Other parameters independent of the coordination number of the zirconium atoms are: (1) the radius of the spherical domain that corresponds to the sphere of volume V_{VDP} , (2) the total area of the surface of the VD polyhedron, and (3) the dimensionless second moment of inertia of the VD polyhedra, which is a parameter characterizing the uniformity of the fluorine arrangement around the Zr atoms. In Table 2, we give the V_{VDP} , R_{sd} , S_{VDP} , and G_3 parameters [20] for the structures of Li_2ZrF_6 at atmospheric conditions ($P\bar{3}1m$, $Z=1$) [2], synthesized at 11 GPa and 1063 K ($P2_1/c$, $Z=4$) [11], and above 10 GPa at room temperature ($C2/c$, $Z=4$) (Table 1 and Fig. 5). The coordination polyhedra around the zirconium atoms in these structures are octahedra, bicapped trigonal prisms, and square antiprisms, respectively. The parameters for the polymorph synthesized at high pressures and temperatures but characterized at atmospheric conditions ($P2_1/c$, $Z=4$) [11] agree perfectly with the ones determined by Serezhkin et al.

[25]. On the other hand, the volume and surface of the Voronoi-Dirichlet polyhedron in the polymorph investigated in this study ($C2/c$, $Z=4$) are smaller than the respective average values due to the compressibility of the bulk volume (Fig. 2), as well as due to the contraction of the Zr–F bonds and the compressibility of polyhedral volumes.

The arrangement of the LiF_6 and ZrF_8 polyhedra in the $C2/c$ phase of Li_2ZrF_6 is very similar to that of TiO_6 and ThO_8 polyhedra in ThTi_2O_6 ($C2/c$, $Z=4$) obtained from the melt [26] or by the solid state reaction at 1473 K [27] and atmospheric pressure. The polymorph of ThTi_2O_6 prepared by the solid state reaction at 1883 K [28] is of the brannerite type ($C2/m$, $Z=4$), in which the O atoms form a near-cubic-close-packing [26]. The brannerite [28] structure contains layers formed by

Table 1

Structural parameters for Li_2ZrF_6 ($C2/c$, $Z=4$) at 14.8 GPa— $a=9.651(6)$ Å, $b=7.533(8)$ Å, $c=4.988(3)$ Å, $\beta=114.94(4)^\circ$, $V=328.8(4)$ Å³

| Atom | Site | x | y | z |
|------------------------|----------|-----------|-----------|------------|
| Li | 8f | 0.255 (7) | 0.536 (9) | 0.576 (15) |
| Zr | 4e | 0.0 | 0.315 (1) | 0.25 |
| F1 | 8f | 0.121 (3) | 0.233 (3) | 0.060 (6) |
| F2 | 8f | 0.395 (4) | 0.041 (3) | 0.350 (6) |
| F3 | 8f | 0.112 (2) | 0.101 (3) | 0.480 (6) |
| Selected distances (Å) | | | | |
| Li–F1 | 2.16 (6) | Li–F1 | 2.65 (7) | |
| Li–F1 | 2.19 (6) | Li–F2 | 2.01 (6) | |
| Li–F2 | 1.74 (6) | Li–F3 | 2.09 (7) | |
| Li–F3 | 1.76 (6) | | | |
| Zr–F1 | 1.89 (2) | (2×) | | |
| Zr–F2 | 2.15 (2) | (2×) | | |
| Zr–F2 | 2.12 (2) | (2×) | | |
| Zr–F3 | 2.02 (2) | (2×) | | |

Estimated standard deviations are given in parenthesis. The symbols (2×) indicate the multiplicity.

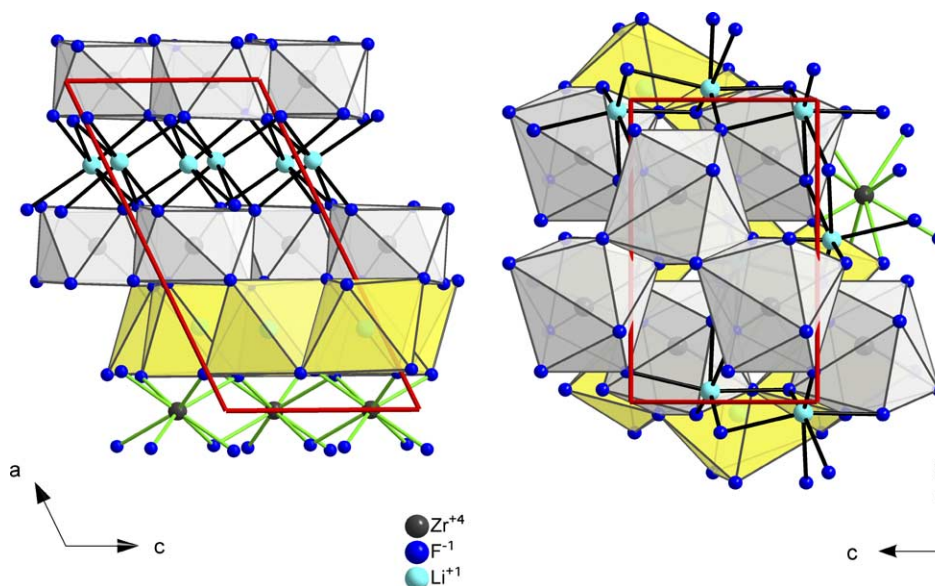


Fig. 4. Crystal structure of Li_2ZrF_6 ($C2/c$, $Z=4$) at 14.8 GPa.

TiO_6 octahedra sharing edges and corners similar to those in the anatase structure parallel to the (101) plane. These octahedra are joined through the thorium atoms in interlayer octahedral positions (Th–O distances of 2.35–2.36 Å). The ThO_6 octahedra are flattened with two more oxygen atoms at 2.96 Å from Th. The eight fold coordination would be a hexagonal bipyramid. Recently, the structures of brannerites $\text{U}_{1-x}\text{M}_x\text{Ti}_2\text{O}_6$ ($M=\text{Ca}$, La , or Gd) [29] as well as of brannerite $\text{U}_{1-x}\text{Y}_x\text{Ti}_2\text{O}_6$ and thorutite $\text{Th}_{1-x}\text{Y}_x\text{Ti}_2\text{O}_{6-\delta}$ [30] have been described in space group $C2/c$ ($Z=4$) in terms of sheets of corner and edge-sharing octahedra TiO_6 in the ab plane separated by eight fold coordinated U/M (U/Y or Th/Y) atoms.

The combined results of this and previous [11] studies on the behaviour of Li_2ZrF_6 show that the mechanism of phase transitions in the A_2BX_6 compounds through cation rearrangements in the octahedral voids of the rigid anion hexagonal close packing array at high pressures and high temperatures as proposed by Galy and Anderson [5] is too limited as it does not account for the coordination changes around the cations and packing of the anions. Depending on the pressure–temperature conditions, Li_2ZrF_6 transforms into polymorphs with the

zirconium atoms either in the bicapped trigonal prisms ($P2_1/c$, $Z=4$) [11] or in the square antiprisms ($C2/c$, $Z=4$) [this study]. In the first case, the fluorine atoms have fluorite-like close packing [12], while in the latter, the fluorine atoms are in the rutile-like close packing. In the context of the P–T phase diagram for the A_2BX_6 compounds, the behaviour of ordered derivatives of the Li_2ZrF_6 type ($P\bar{3}1m$, $Z=1$) [7,8] provides additional information. The structure of $\text{LiSrAlF}_6\text{-II}$ ($P2_1/c$, $Z=4$), stable between 1.6 and 3.0 GPa, is a distorted derivative of the ambient pressure polymorph ($\text{LiSrAlF}_6\text{-I}$, $P\bar{3}1c$, $Z=2$) with the cations exclusively in deformed octahedral coordinations [13]. LiCaAlF_6 transforms to this monoclinic polymorph II above about 7 GPa. $\text{LiSrAlF}_6\text{-III}$, occurring above 3.0 GPa, is related to the LiBaCrF_6 structure ($P2_1/c$, $Z=4$) and is built of deformed SrF_{12} icosahedra within a three-dimensional framework of corner-sharing distorted AlF_6 octahedra and LiF_4 tetrahedra [14]. The pressure-induced changes of the coordination polyhedra in the series $\text{LiSrAlF}_6\text{-I}$, $\text{LiSrAlF}_6\text{-II}$, to $\text{LiSrAlF}_6\text{-III}$ are thus similar to the differences in coordination polyhedra due to the increase of the ionic radii of the Sr^{+2} and Ba^{+2} cations in $\text{LiSrAlF}_6\text{-I}$ and $\text{LiBaM}''\text{F}_6$

Table 2

The V_{VDP} , R_{sd} , S_{VDP} , and G_3 parameters characterizing the Voronoi–Dirchlet polyhedra [16] in the structures of Li_2ZrF_6 at atmospheric conditions ($P\bar{3}1m$, $Z=1$) [2], synthesized at 11 GPa and 1063 K ($P2_1/c$, $Z=4$) [9], and above 10 GPa at room temperature ($C2/c$, $Z=4$) (Table 1)

| Polymorph | Coord. No. | V_{VDP} , (Å ³) | R_{sd} , (Å) | S_{VDP} , (Å ²) | G_3 |
|----------------------|------------|--------------------------------------|------------------------|--------------------------------------|--------------------------|
| $P\bar{3}1m$, $Z=1$ | 6 | 8.03 <i>8.1(4)</i> | 1.24 <i>1.24(2)</i> | 24.06 <i>24.2(7)</i> | 0.083 <i>0.084(1)</i> |
| $P2_1/c$, $Z=4$ | 8 | 8.05 | 1.24 | 22.80 | 0.082 |
| $C2/c$, $Z=4$ | 8 | 7.53 <i>7.9(2)</i> | 1.24 <i>1.24(1)</i> | 22.02 <i>22.5(3)</i> | 0.083 <i>0.081(1)</i> |

They are compared with the average values for a given coordination number in all zirconium-containing fluorides at atmospheric pressure [21] (in italics). The corresponding values of the V_{VDP} , R_{sd} , S_{VDP} , and G_3 parameters for all fluorides disregarding the actual coordination numbers of the zirconium atoms are 8.0(2) Å³, 1.24(1) Å, 23.1(8) Å², and 0.082(1), respectively [21].

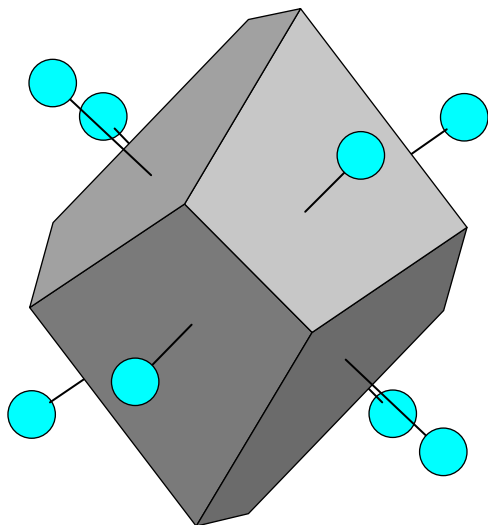


Fig. 5. Voronoi-Dirichlet polyhedron around the zirconium atoms in Li_2ZrF_6 ($C2/c$, $Z=4$) at 14.8 GPa.

($M'' = \text{Al, Ga, Cr, V, Fe, or Ti}$) at ambient conditions. The pressure-induced coordination changes in the $\text{LiM}'\text{M}''\text{F}_6$ compounds ($P\bar{3}1c$, $Z=2$; $M' = \text{Ca or Sr}$; $M'' = \text{Al, Ga, or Cr}$) are expected to yield the materials with higher cross sections for dopant optical emissions [7,13,14].

5. Concluding remarks

Submitting dilithium zirconium hexafluoride Li_2ZrF_6 to a pressure higher than 10 GPa at room temperature has produced a monoclinic crystal structure ($C2/c$, $Z=4$) with the lithium and zirconium atoms in distorted octahedral and square antiprism coordinations to fluorines, respectively. This new structure is different from the one ($P2_1/c$, $Z=4$) synthesized previously at 11 GPa and 1063 K and studied in its quenched state [11]. In that structure, the polyhedra around the zirconium atoms are edge-sharing bicapped trigonal prisms along the a -axis, while the Li–F coordination polyhedra at two non-equivalent Li^{+1} sites are square pyramids. In the present $C2/c$ structure, the fluorine atoms have rutile-like close packing, whereas in the former $P2_1/c$ one [11], the fluorine atoms are in the fluorite-like close packing.

Our study emphasizes the need for extensive and systematic investigations of pressure-induced crystal structures in this and related A_2BX_6 -type materials to clarify the details of the mechanisms for their phase transformations and of their P–T phase diagrams.

Acknowledgements

Experimental assistance from the staff of the Swiss-Norwegian Beamlines at ESRF is gratefully acknowledged.

Several discussions with T. Balić-Žunić helped us better understand crystal chemistry of the A_2BX_6 -type compounds. We thank J.-Y. Gesland for providing the sample of Li_2ZrF_6 . AG acknowledges financial support from the Ministerio de Ciencia y Tecnología and Ministerio de Educación y Cultura. HPW acknowledges continuous financial support from the Swiss National Foundation (Berne) and the Tisserand Foundation (Montrichet).

References

- [1] R. Hoppe, W. Dahne, *Naturwissenschaften* 47 (1960) 397.
- [2] G. Brunton, *Acta Crystallogr.* B29 (1973) 2294.
- [3] B.G. Hyde, B.G. Hyde, S. Andersson, *Inorganic Crystal Structures*, Wiley, New York, 1989.
- [4] U. Müller, *Z. Anorg. Allg. Chem.* 624 (1998) 529.
- [5] J. Galy, S. Andersson, *J. Solid State Chem.* 3 (1971) 525.
- [6] J.M. Leger, J. Haines, *Eur. J. Solid State Inorg. Chem.* 34 (1997) 785.
- [7] K.I. Schaffers, D.A. Keszler, *Acta Crystallogr. C* 47 (1991) 18; Y. Yin, D.A. Keszler, *Chem. Mater.* 4 (1992) 645.
- [8] D. Babel, *Z. Anorg. Allg. Chemie* 406 (23) (1974); D. Babel, *Z. Anorg. Allg. Chemie* 406 (1974) 38.
- [9] T. Sekino, T. Endo, T. Sato, M. Shimada, *J. Solid State Chem.* 88 (1990) 505.
- [10] B. DeBoer, R.A. Young, A. Sakthivel, *Acta Crystallogr. C* 50 (1994) 476.
- [11] A. Grzechnik, J.-Y. Gesland, *Z. Krist. NCS* 218 (2003) 3.
- [12] Y. Lalignat, A. Le Bail, G. Ferey, D. Avignant, J.C. Cousseins, *Eur. J. Solid State Inorg. Chem.* 25 (1998) 551; M. Guillot, M. El-Ghozzi, D. Avignant, G. Ferey, *J. Solid State Chem.* 97 (1992) 400.
- [13] A. Grzechnik, V. Dmitriev, H.-P. Weber, J.-Y. Gesland, S. van Smaalen, *J. Phys. Condens. Matter* 16 (2004) 1033.
- [14] A. Grzechnik, V. Dmitriev, H.-P. Weber, J.-Y. Gesland, S. van Smaalen, *J. Phys. Condens. Matter* 16 (2004) 3005.
- [15] A.P. Hammersley, S.O. Svensson, M. Hanfland, A.N. Fitch, D. Häusermann, *High Press. Res.* 14 (1996) 235.
- [16] G.J. Piermarini, S. Block, J.D. Barnett, R.A. Forman, *J. Appl. Phys.* 46 (1975) 2774; H.K. Mao, J. Xu, P.M. Bell, *J. Geophys. Res.* 91 (1986) 4673.
- [17] A. Boulif, D. Louer, *J. Appl. Crystallogr.* 24 (1991) 987.
- [18] J. Laugier, B. Bochu, CHEKCELL, <http://www.inpg.fr/LMGP>
- [19] H. Putz, J.C. Schön, M. Jansen, *J. Appl. Cryst.* 32 (1999) 864.
- [20] V.A. Blatov, A.P. Shevchenko, *Acta Crystallogr. A* 59 (2003) 34.
- [21] E.V. Peresypkina, V.A. Blatov, *Acta Crystallogr. B* 59 (2003) 361.
- [22] A.C. Larson, R.B. von Dreele, *GSAS: General Structure Analysis System*, Los Alamos National Laboratory, 2000.
- [23] P.W. Stephens, *J. Appl. Crystallogr.* 32 (1999) 281.
- [24] A.F. Wells, *Structural Inorganic Chemistry*, fifth ed., Oxford University Press, Oxford, 1984.
- [25] V.N. Serezhkin, V.A. Blatov, E.S. Kuklina, *Russ. J. Coord. Chem.* 22 (1996) 605.
- [26] T. Balić-Žunić, S. Ščavničar, Z. Grobnski, *Croatica Chem. Acta* 57 (1984) 645.
- [27] O. Loye, M.P. Laruelle, A. Harari, *C.R. Acad. Sci. Paris, Série* 266 (1968) 454.
- [28] R. Ruh, D. Wadsley, *Acta Crystallogr.* 21 (1966) 974.
- [29] M. James, N. Watson, *J. Solid State Chem.* 165 (2002) 261.
- [30] M. James, M.L. Carter, N. Watson, *J. Solid State Chem.* 174 (2003) 329.